# Three-Dimensional Internet-of-Things Deployment With Optimal Management Service Benefits for Smart Tourism Services in Forest Recreation Parks

**CHUN-CHENG LIN [1], (Senior Member, IEEE), WAN-YU LIU [2,3], AND YU-WEN LU [1]**

[1]Department of Industrial Engineering and Management, National Chiao Tung University, Hsinchu 300, Taiwan
[2]Department of Forestry, National Chung Hsing University, Taichung 402, Taiwan
[3]Innovation and Development Center of Sustainable Agriculture, National Chung Hsing University, Taichung 402, Taiwan

Corresponding author: Wan-Yu Liu (wyliu@nchu.edu.tw)

**ABSTRACT** In a large-scale national forest recreation park, it is difficult for park managers to maintain facilities and provide timely or emergency services to visitors in need (e.g., elderly adults, children, or lost visitors without communication devices). To implement smart tourism services, park managers have introduced the Internet of things (IoT) to their parks, which has enabled the provision of diversified intelligent information services. However, most of the previous studies focused on 2D deployment of the IoT system to cover all targets, ignoring actual 3D topographic differences; their objectives rarely included the effectiveness of services generated from introducing the IoT; they assumed targets to be equally crucial, regardless of differences in tourism attractiveness (e.g., tourist attractions, view trails, and recreation facilities). Therefore, this study investigates 3D deployment of an IoT system to cover targets with different scores based on tourism attractiveness in a forest recreation park with optimal management service benefits, represented as a weighted sum of service quality index (SQI) and managerial setting attributes index (MSAI), so that the system collects the data from visitors equipped with wearable devices, and applies it to tasks such as physiological detection and positioning. This problem belongs to deployment and coverage problems, which have been shown to be NP-hard, and thus is also NP-hard. Therefore, this study further solves this problem by improved simulated annealing (ISA), including three neighborhood searching operators and the dynamic probability adjustment scheme. Experimental results under various parameter settings indicate that ISA has an excellent optimization ability.

**INDEX TERMS** Smart tourism service, Internet of Things, simulated annealing, three-dimensional deployment, national forest recreation park.

## I. INTRODUCTION

The travel and tourism industries have been flourishing in recent years, and the technological cooperation between tourism and information technology (IT) has also matured. In smart tourism services, IT such as Internet of things (IoT) [1], radio frequency identification (RFID), wireless sensor networks (WSNs), and near-field communication (NFC) has been used to provide tourists with accurate travel information and rich travel experiences [2], [3]. For example, tourists may download a recreation park's app and book time slots for their rides or facilities. This can shorten visitors' waiting time spent in queues as well as improve facilities' overall usage rate and visitors' satisfaction.

Visitors enjoy local art and culture, festivities and activities, and nature and ecosystems. Nature-based tourism [4] is a rapidly growing sector of the tourism industry. The main goals of visitors are to experience the natural environment and feel natural phenomena such as topographic, hydrographic, and forest landscapes. Tourists have increasingly been

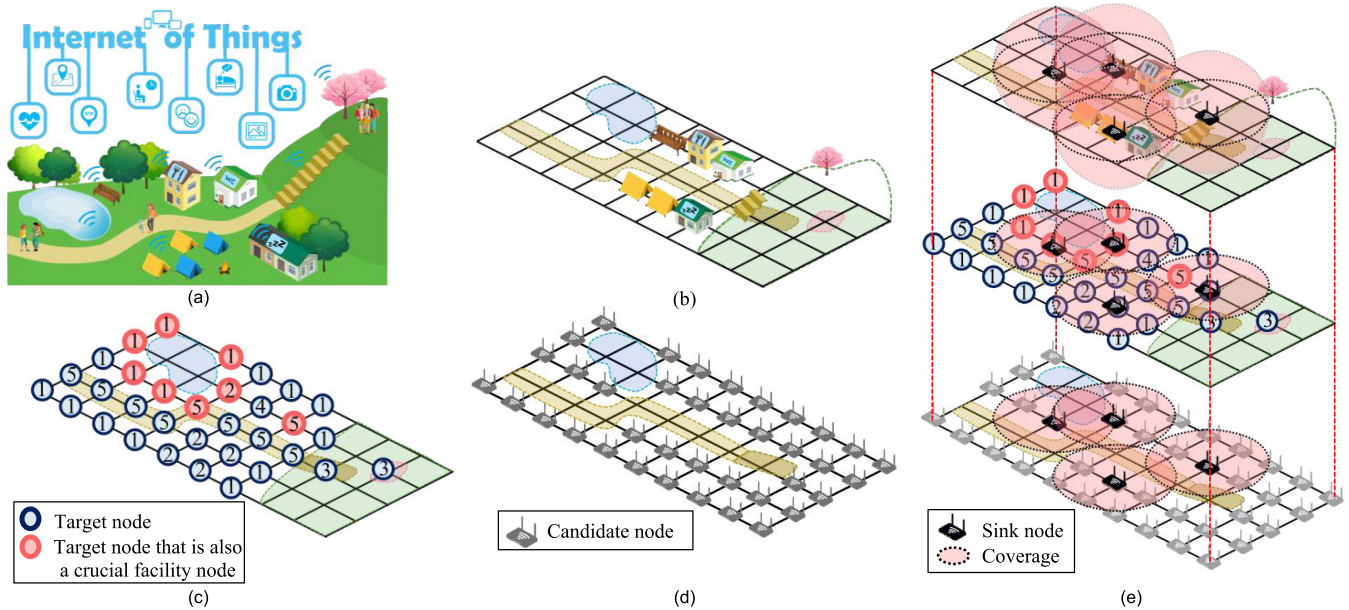The associate editor coordinating the review of this manuscript and approving it for publication was Guanjun Liu.

**FIGURE 1.** (a) Illustration of 3D deployment of an IoT system in a forest recreation park. (b) The park is projected to a 2D grid with a 3D underling space. (c) Target nodes, including crucial facility nodes. (d) Candidate nodes which can be deployed with sink nodes. (e) A solution with deployment of four sink nodes.

escaping from the city and travelling to the countryside to walk and relax both physically and psychologically. Forest recreation parks have natural landscape ecologies; they enable visitors to experience the natural environment and engage in leisure, sports, and entertainment activities, which have led to a gradual increase in the number of visitors to forest recreation parks. However, forest recreation parks have a large scope and can be difficult to manage, and thus fail to satisfy visitors' needs in a timely manner. For example, such parks cannot provide timely services to (1) elderly adults, children, or visitors who become separated from their group and do not have a communication device, (2) emergency services to visitors who suddenly become ill, and (3) prompt cleaning services to dirty facilities. Therefore, forest park managers have sought to transform their business models into recreation parks characterized y smart tourism, to increase visitors' satisfaction and their willingness to revisit.

To implement smart tourism services, forest park managers have introduced IoT systems to their parks. Specifically, they deployed wired or wireless *sink nodes* (which are the devices to which the data collected is sent) to cover various types of *targets* (e.g., tourist attractions, viewing trails, and recreation facilities) in their parks. Visitors were equipped with wearable devices (e.g., wristbands, medical bands, smartwatches, smart glasses, and so on), or carried smartphones or other smart devices; facilities in parks were equipped with sensor devices. The data (e.g., location, heartbeat, blood pressure, sleep quality, usage frequency, and user survey) of visitors and facilities collected by sink nodes through the IoT system was sent to the cloud center of the system for operational analysis to provide various smart services and applications, and was applied immediately to provide timely diversified

services (e.g., timely search and rescue, warning reminder, sedentary reminder, interactive environmental explanation, interactive recreation games, human-computer interaction with facilities, social media check-ins, and augmented-reality image/video) to increase visitors' satisfaction and their willingness to revisit (Figure 1(a)). The IoT has a wide range of applications and can achieve the benefits of immediate response, information integration, and proactive services. Introducing the IoT to travel destinations can enable the future sustainable growth of tourist attractions; additionally, integrating visitor interactions and environmental facilities can enhance the quality of travel experiences in destinations (Gretzel et al., 2015).

Most related studies had the following four features. Firstly, most studies focused on deployment of the IoT system that optimizes various objectives such as the number of deployments, coverage of targets, system survival lifetime, and energy consumption [5]. Secondly, most studies investigated deployment of IoT systems in 2D spaces, regardless of actual 3D topographic differences. Consequently, even though the deployment results had optimized a certain objective on a 2D plane, they might not be implemented in real 3D environments. For instance, a region covered by a sink node on a 2D plane may not be covered by this sink node according to actual 3D topographic differences. Thirdly, most studies assumed all targets to be equally crucial. That is, they did not assign different scores to various targets according to the usage frequency of these targets. Consequently, when deploying a limited number of sink nodes in a forest recreation park, some crucial tourist attraction targets may not be covered. Therefore, the importance of the characteristics of each target should be identified by users, and scores should be

set according to the information of targets, thereby increasing the precision of sink-node deployment [6]. Fourthly, most studies rarely investigated the service level index [7]. This index evaluates the service quality of IoT deployment systems; furthermore, it examines whether the range covered by the IoT deployment was the regions that park managers wish to manage, thereby enhancing service quality. Additionally, to meet park managers' expectations, adjustments were made to parameters related to the service level index, such as the number of sink nodes, distance between them, and scores of landscapes.

In light of the above, this study investigates 3D deployment of an IoT system in a forest recreation park with optimal management service benefits, so that the system can collect the data from visitors equipped with wearable devices, and apply it to tasks such as physiological detection and positioning. First, this study represents a 3D national forest recreation park as a 2D grid (Figure 1(b)), in which each grid point is assigned with a score according to visitor flows and tourism attractiveness (e.g., tourist attractions, viewing trails, and recreation facilities). Those grid points with non-zero score are target nodes; furthermore, some of the target nodes are crucial facility nodes emphasized by the park managers (Figure 1(c)), so that the deployment result will be influenced by the park managers according to their management service benefits. Then, according to 3D topographies and actual facilities in the park, a part of the grid points are the candidate nodes that could be placed by sink nodes (Figure 1(d)).

The problem concerned in this study is to find the candidate nodes that are deployed with sink nodes, so as to optimize a weighted sum of the following two management service indices proposed in this study: service quality index (SQI) and managerial setting attributes index (MSAI), which are used to evaluate the total score of the covered area and the crucial facilities (e.g., toilets, trails, and specific tourist attractions), respectively. With the two indices, the park managers could provide timely facility maintenance services through the IoT system, further improving visitors' satisfaction. Furthermore, this study considers the collision problem between multiple sink nodes and IoT tags attached to visitors [8], [9]. Specifically, the collision problem refers to a signal interference caused by overly short distances between sink nodes. When a tag is located in the identification zone of two sink nodes simultaneously, the IoT tag is read by multiple sink nodes, resulting in imprecise positioning of the label. To prevent the collision problem, the distance between sink nodes cannot be set to be less than a specified minimum distance.

This study first models the concerned problem as a binary integer programming model, which is NP-hard. Additionally, relevant studies have showed deployment and coverage problems to be NP-hard (e.g., [10], [11]), and thus the concerned problem is also NP-hard. Therefore, this study solves the concerned problem by the improved simulated annealing (ISA) algorithm, which employs three neighborhood searching operators to increase the diversity of searching neighborhoods, and dynamically adjusts the probabilities of selecting

one of the three operators in each iteration through a dynamic selection probability adjustment scheme. The main contributions of this study were as follows:

- Different from most studies that deployed IoT systems in 2D spaces, this study solves the problem of deploying an IoT system after 3D topographic differences and tourist attractions are considered.
- Different from most studies that assume all targets to be equally crucial, the problem model assigns different scores to tourist attractions according to their tourism attractiveness and crucial facilities. Moreover, topographic limitations, coverage problem, and collision problem are considered.
- This study proposes the SQI and MSAI, thereby achieving the optimal sink-node coverage of regions with visitor flows. Moreover, it considers crucial facilities emphasized by park managers and helps managers to select optimal deployment positions.

The remainder of this study is organized as follows. Section 2 presents a literature review on deployment problems and the factors affecting the attractiveness of forest recreation parks. Section 3 describes the overall framework of the concerned IoT system deployed in forest recreation parks, describes the concerned problem, and creates a mathematical programming model for the problem. Section 4 presents the proposed ISA algorithm in detail. Section 5 presents implementation of the proposed ISA and conducts experimental analysis. Finally, Section 6 presents the conclusions with future works.

## II. LITERATURE REVIEW

It is of importance to investigate how to deploy sink nodes in the perception layer of an IoT system. Effective deployment can reduce costs and increase the quality of perceptions in the system. This section reviews deployment problems of sink nodes that optimize various objectives, 3D deployment problems, and the previous studies on analyzing factors affecting the attractiveness of forest recreation parks.

### A. DEPLOYMENT PROBLEMS OPTIMIZING VARIOUS OBJECTIVES

Rebai *et al.* [12] investigated how to deploy the minimum number of wireless sensors to cover the concerned geographical region, under the constraint with connectivity between sensors. Khoufi *et al.* [13] not only considered the constraints of the coverage range and connectivity, but also emphasized the importance of energy consumption. Specifically, they first deployed sensor nodes and receivers, and then scheduled the activities of sensor nodes. Sengupta *et al.* [5] investigated a multi-objective problem that considers the tradeoff among maximization of the covered range, maximization of network lifetime, and minimization of energy consumption. Similarly, Maheshwari and Chand [14] investigated the multi-objective problem that considers maximization of covered range, maximization of network lifetime, and minimization of the

number of sensors. Farsi *et al.* [15] integrated the problems of maximizing the network lifetime, the covered range, and connectivity of WSNs; additionally, they compared the advantages and disadvantages of different WSNs.

Mini *et al.* [16] solved WSN deployment problems that considers optimization of different types of target coverage (i.e., simple cover, k-cover, and Q-cover); moreover, they used the artificial bee colony (ABC) algorithm to identify optimal deployments in 3D topographies. Mini *et al.* [17] investigated a bi-objective problem of deploying WSNs, and used the ABC algorithm to first deploy sensors with weights based on sensor battery power, and then to plan a schedule of switching on/off sensors, to achieve the maximum network lifetime. Sitanayah [18] measured the importance of sensor nodes on transmission efficiency, and then deployed the WSN according to the ranking of importance, increasing the stability of the WSN.

Tsai *et al.* [7] investigated the optimal deployment of RFID readers with the objective of maximizing the coverage rate and minimizing the weight of the collision chance of readers; additionally, they evaluated the quality of service (QoS) of the SQI of the system [19].

### B. THREE-DIMENSIONAL DEPLOYMENT PROBLEMS

Hervert-Escobar *et al.* [20] considered the interference of obstacles in 3D warehouses, achieving coverage of all target objects using the minimum number of RFID readers. Lin *et al.* [21] proposed an IoT simulation model based on Zigbee, and discussed the effect of various topographies, data loadings, and node velocities on the performance of WSNs in 3D spaces. They consulted the aforementioned research on 3D deployments, and employed them as their deployment method. Cao *et al.* [22] deployed WSNs in 3D industrial spaces considering optimization of the covered range and the WSN lifetime. Naveen *et al.* [23] deployed a WSN in a 3D virtual grid with the objective of prolonging the WSN lifetime. Qasim *et al.* [24] used ant colony optimization (ACO) to deploy a WSN in a 3D grid with the objective of minimizing cost. Mnasri *et al.* [25] used a multi-objective optimization algorithm based on dominance and decomposition (MOEA/DD) to solve problems regarding the deployment of WSNs in indoor 3D virtual spaces.

### C. ANALYZING FACTORS AFFECTING THE ATTRACTIVENESS OF FOREST RECREATION PARKS

To reflect the real situation, this study considers that tourist attractions have different importance, based on which the optimal deployment of sink nodes in the park is determined. Table 1 indicates the categorization of factors affecting the tourism attractiveness of forest recreation parks in the previous studies. Deng *et al.* [26] and Lee *et al.* [27] conducted hierarchical structural analysis [28] on factors affecting the tourism attractiveness of forest recreation parks [29]. Wang *et al.* [30] extracted keywords from Internet platforms, and investigated factors affecting the attractiveness of each location and landscape in forest recreation parks through

**TABLE 1.** Factors affecting the attractiveness of forest recreation parks in the previous studies.

| Reference | Factors |
|---|---|
| Deng et al. (2002) | Forest landscapes, recreational and educational facilities, accessibility, local community culture, and surrounding tourist attractions |
| Lee et al. (2010) | Forest attractions and landscapes, climate conditions, and accommodation and dining |
| Wang et al. (2018) | Forest landscapes, cost/time consumption, recreational and educational facility/activity, surrounding tourist attractions, and cultural factors |
| Markowski et al. (2019) | Animal/plant diversity, history and culture, accommodation and dining, entertainment activities, and accessibility |

semi-open questionnaires. Similarly, Markowski *et al.* [31] organized 30 factors affecting the tourism attractiveness of Vietnamese national parks.

### D. DISCUSSION

Most studies on deploying the IoT (or WSN, or RFID readers) have focused the following objectives: the system deployment cost, coverage maximization, hardware system lifetime, and energy consumption. However, the effectiveness of services generated by the introduction of the IoT to forest recreation parks has rarely been discussed. Studies have mostly deployed the IoT in 2D spaces and ignored actual topographic differences. Forest recreation parks must be deployed in 3D spaces to better conform to reality. The previous studies on coverage maximization have assumed all objectives to be equally crucial, and thus failed to consider differences in tourism attractiveness. Consequently, some crucial tourist attractions may not be covered when considering deploying a limited number of sink nodes in forest recreation parks.

The problem model in this study considers the following features:

- This model considers 3D topographic differences and limitations to deploy sink nodes in 3D spaces.
- This model assigns different scores to different facilities in the park according to tourism attractiveness and crucial facilities.
- This model considers the interference problem caused by signal collisions between sink nodes.
- This model proposes the SQI and MSAI based on tourists' preferences and managers' managerial decisions.

## III. PROBLEM DESCRIPTION

This section first gives the overall framework of the IoT system deployed in forest recreation parks, then describes the problem setting, and then creates a mathematical programming model for this problem.

### A. SYSTEM FRAMEWORK

This study considers deploying an IoT system in a forest recreation park. The IoT system is separated into the following three layers: (1) Perception layer: This layer includes two

types of devices: wearable device and sink node. Each visitor to the park is asked to be equipped with a wearable device, which is a sensor or a smart device. Sink nodes are deployed in the park, and are used to collect data from wearable devices on visitors. Each sink node has a wireless coverage, and it gathers data collected by the wearable devices within its coverage. (2) Network layer: This layer receives data collected in the perception layer, and sends it to the application layer. (3) Application layer: This layer conducts data integration and analysis, and applies the results to the forest recreation park. This study considers the following applications in forest recreation parks:

- Landscape interactions: Tourist attractions can be integrated with their local music, arts, and the Internet. Additionally, human-computer interaction (HCI) devices can be set up to interact with visitors, so that greater exchanges and memorable travel experiences can be created when visitors are interacting with tourist attractions. Moreover, this achieves the effect of marketing and may attract new visitors.
- Physiological detection: Most visitors travel to forest recreation parks in the hope of obtaining health benefits. Therefore, through wearable devices, visitors can check their own physiological data, including heartrate, blood pressure, blood oxygen, step count, calories consumed, and a reminder when individuals sit for a long time.
- Positioning: If visitors encounter an emergency (e.g., elderly adults or children getting lost) and do not have communication devices, it is difficult to search for them in a short time because the forest park area is large. Alternatively, when emergency services are required for visitors who suddenly become ill, they can be tracked and helped through positioning.
- Game mechanism: Forest landscapes have seasonal changes, and forest park managers may propose thematic activities accordingly. Specifically, park managers may hold point collection activities using trails or landscapes. This can be indirectly used to recommend suitable travel itineraries for a particular season to visitors and enable them to experience diverse travel itineraries. Augmented reality (AR) [32] is the synchronous display of virtual 3D objects and the actual environment through mobile devices, such as smartphones or tablets. If AR stations were set up in less popular tourist attractions, visitors would be encouraged to complete tasks and visit more tourist attractions; this can be achieved through enabling integration and interactions between virtual objects and attractions in reality. In addition to providing the aforementioned IoT applications, park managers could obtain visitor data from wearable devices and feedback from the aforementioned applications; for example, the walking route of visitors, highly crowded regions, and rarely visited tourist attractions. Management policy can be adjusted based on valuable information obtained through IT [33], [34].

Sink nodes could be wired or wireless. In practice, a forest recreation park generally provides wired roadside lights to visitors in the neighborhood of both target nodes and crucial facility nodes. Therefore, this study assumes that sink nodes are connected with roadside lights by wires, and hence their power is supported by the same energy source with the roadside lights. Note that if recharging sink nodes is concerned, it requires the cost of acquiring recharging facilities and the cost of maintaining these facilities. In the future, it would be of interest to investigate the recharging management of sink nodes, or the sink nodes equipped with the function of harvesting renewable energy.

## B. PROBLEM SETTING AND DESCRIPTION

At the park entrances, the park staff distribute a wearable device to each visitor. Suppose that wearable devices have uniform specifications; and there are no interferences from system malfunctions or environmental factors (metal and water). The problem concerned in this study is concerned about determining a 3D deployment of an IoT system (i.e., determining positions of a number of sink nodes) to cover targets with different scores based on tourism attractiveness and crucial facilities emphasized by park managers in a forest recreation park, to collect tourist information and further to provide diversified IoT applications.

Consider a forest recreation park in a 3D space (Figure 1(a)), in which tourist attractions are mostly flat regions. This study first maps this 3D park to a 2D map represented as a grid (Figure 1(b)) with $H \times W$ grid points. Then, according to the information on the visitor flow of each place as well as locations of tourist attractions in the park, the park managers set a subset of these grid points as *target nodes* (Figure 1(c)), and they assign each target node a *score* to reflect the degree of importance, tourism attractiveness, and crucial facilities. For example, in Figure 1(c), both blue and red nodes on the map represent target nodes, and red target nodes further represent crucial facilities (e.g., toilets and specific tourist attractions), which are emphasized by park managers. Note that the grid points on the right side of the map are not target nodes, because visitors cannot enter these grid points. Additionally, the number attached to each target node is its score decided by the park managers. Also note that some target nodes for crucial facilities (i.e., red target nodes in Figure 1(c)) may not be assigned a high score by park managers, because park managers might see the potential for development in currently unpopular tourist attractions or focusing on regions that will be developed.

To deploy an IoT system (i.e., to place sink nodes to cover target nodes) in the park, this study selects a subset of grid points in the map grid as the *candidate nodes* in which sink nodes could be placed according to the condition that the actual topographies of 3D spaces cannot be seen in 2D grid nodes, such as steep slopes and cliff surroundings (Figure 1(d)). In addition, grid points with limited places cannot serve as candidate nodes, e.g., those in the middle of entrances and trails.

With the above problem setting, the problem in this study is to deploy a number of sink nodes (each of which has a wireless coverage range, which can be regarded as a 3D sphere in the 3D park space) on candidate nodes to cover target nodes, with the objective of maximizing managerial service benefits, consisting of service quality index (SQI) and managerial setting attributes index (MSAI) in terms of the scores of target nodes (Figure 1(e)), subject to the following constraints:

- Constraint of the maximal score sum of the target nodes covered by each sink node: Because a target node with a higher score needs to serve more visitors (i.e., to collect more visitor information), this constraint is added to prevent one single sink node from receiving excessive information, which could overload the system.
- Constraint of collision avoidance between sink nodes (or the distance constraint between sink nodes): The minimum 3D distance (MD) between sink nodes is set because overly short distances would result in collisions that cause signal interferences.

## C. MATHEMATICAL PROGRAMMING MODEL

The notation used in the mathematical programming model of the concerned problem is given in Table 2.

**TABLE 2.** Notation used in the problem model.

| Index | Definition |
|---|---|
| $i, j$ | Indices of candidate nodes. |
| $k$ | Index of a target node. |
| $l$ | Index of a crucial facility node. |

| Parameter | Definition |
|---|---|
| $G$ | Number of grid points. |
| $N$ | Number of candidate nodes. |
| $T$ | Number of target nodes. |
| $F$ | Number of crucial facility nodes. |
| $x_i$ | Notation of the $i$th candidate node, for $1 \leq i \leq N$. |
| $t_k$ | Notation of the $k$th target node, for $1 \leq k \leq T$. |
| $f_l$ | Notation of the $l$th crucial facility node, for $1 \leq l \leq F$. |
| $\omega$ | Weight of the SQI in the objective function, for $0 \leq \omega \leq 1$. |
| $R$ | Radius of the sensing coverage of each sink node. |
| MD | Minimum 3D distance between sink nodes, which is no greater than $2R$. |
| $Q$ | Maximal number of sink nodes that can be deployed. |
| $U$ | The maximal score sum of all target nodes covered by a sink node. |
| $S(t_k)$ | Score of target node $t_k$, for $k \in \{1, 2, …, T\}$. |
| $S_{th}$ | The score threshold used for canceling the distance constraint between sink nodes. |
| $d(\cdot, \cdot)$ | 3D Euclidean distance between two nodes. |

| Decision variable | Definition |
|---|---|
| $X_i$ | $X_i = \begin{cases} 1, & \text{if a sink node is deployed on candidate node } x_i; \\ 0, & \text{otherwise.} \end{cases}$ |

| Response variable | Definition |
|---|---|
| $G_{ki}$ | $G_{ki} = \begin{cases} 1, & \text{if target node } t_k \text{ is covered by a sink node deployed} \\ & \text{on candidate node } x_i \text{ if the sink node exists;} \\ 0, & \text{otherwise.} \end{cases}$ |
| $C_k$ | $C_k = \begin{cases} 1, & \text{if target node } t_k \text{ is covered by some sink node;} \\ 0, & \text{otherwise.} \end{cases}$ |
| $\lambda_{ij}$ | $\lambda_{ij} = \begin{cases} 1, & \text{if at least one of the scores of the two target nodes} \\ & \text{corresponding to candidate nodes } x_i \text{ and } x_j \text{ is no less} \\ & \text{than threshold } S_{\text{limit}}; \\ 0, & \text{otherwise.} \end{cases}$ |

The problem concerned in this study is modeled as a binary integer programming model, which is detailed as follows. Consider a park represented as a grid consisting of $G = H \times W$ grid points. Among the $G$ grid points, $N$ grid points are candidate nodes for deployment of sink nodes (denoted by $x_1, x_2, \ldots x_i, \ldots, x_N$); $T$ grid points are target nodes (denoted by $t_1, t_2, \ldots, t_k, \ldots, t_T$). Among the $T$ targets nodes, $F$ target nodes are crucial facilities nodes emphasized by park managers (denoted by $f_1, f_2, \ldots, f_l, \ldots, f_F$). Note that $N \leq G$; $F \leq T \leq G$. Note that the $N$ candidate nodes and the $T$ target nodes may not be disjoint (i.e., some target nodes and candidate nodes refer to the same grid point).

Let $S$ denote the score function of a target node (or a crucial facility node). That is, the score of target node $t_k$ is $S(t_k)$; and the score of crucial facility node $f_l$ is $S(f_l)$.

The problem concerned in this study is to place at most $Q$ sink nodes on the $N$ candidate nodes to maximize managerial service benefits consisting of SQI and MSAI as follows:

$$\text{Maximize } \omega \cdot \text{SQI} + (1 - \omega) \cdot \text{MSAI} \quad (1)$$

where $\omega$ controls the weight of the two indices, and can be adjusted according to park managers' needs.

The SQI is evaluated as follows:

$$\text{SQI} = \frac{\text{TCS}}{\sum_{k=1}^{T} S(t_k)} \cdot \frac{\text{MD}}{2R} \quad (2)$$

where TCS is the sum of all target scores of the candidate nodes covered by sink nodes (i.e., within the coverage of sink nodes), which is calculated as follows:

$$\text{TCS} = \sum_{k=1}^{T} C_k \cdot S(t_k) \quad (3)$$

where $C_k$ is a binary variable for determining whether target node $t_k$ is covered by some sink node; MD is the minimum 3D distance between sink nodes; and $R$ is the radius of the sensing coverage of each sink node. In the right side of Eq. (2), the first fraction is a normalized TCS; and the second fraction is used for collision avoidance. A greater MD/2$R$ value means that collisions between sink nodes are not allowed, and thus, the SQI is expected to be more important than the MSAI in the objective function.

When the SQI value is greater, maximum coverage is achieved without minimal collisions between sink nodes. This indicates that managers can receive more precise information and make superior decisions when the precision of sensing is higher. Note that the SQI in this study is different from the SQI proposed in [7], which only considered the maximization of coverage but not collision problems between sink nodes.

The MSAI is a normalized TFS as evaluated as follows:

$$\text{MSAI} = \frac{\text{TFS}}{\sum_{l=1}^{F} S(f_l)} \quad (4)$$

where TFS is the sum of the scores of all crucial facility nodes covered by sink nodes, which is calculated as follows:

$$\text{TFS} = \sum_{l=1}^{F} C_{\mu(f_l)} \cdot S(f_l) \quad (5)$$

where $\mu$ is a function mapping from a crucial facility node to the corresponding target node. That is, for each $l \in \{1, 2, \ldots, F\}$, crucial facility node $f_l$ is mapped to target node $t_k = \mu(f_l)$ for a certain index $k \in \{1, 2, \ldots, T\}$, so that crucial facility node $f_l$ and target node $t_k$ are the same grid point on the map grid.

When the TFS value is greater, the coverage rate of crucial facility nodes would be higher. For example, places such as toilets, specific tourist attractions, and trails should have high score values to provide precise visitor information and enable park managers to provide services that are more congruent with visitors' feelings or provide timely facility maintenance. For this concept, we consulted the work in [35], who proposed that visitors were influenced by the environment when engaging in recreational activities; and therefore, managers' management decisions would affect the recreational environment, further affecting visitors' experiences and feelings. Park managers' efforts to manage the natural environment, retain its original appearance, and hold recreational activities can improve a park's tourism attractiveness and competitiveness. Furthermore, park managers' efforts to create an excellent recreational region and enable tourists to have high-quality nature experiences would increase visitors' satisfaction [36]. Therefore, this study not only considers visitor preferences (in terms of visitor flows) but also adds park managers' management decisions (i.e., we add the concept that the regions emphasized by park managers are crucial facilities).

With the objective function (1), the problem model is subject to Constraints (6)–(11). Because the park range is broad, park managers could only deploy a limited number of sink nodes. Therefore, Constraint (6) enforces that the number of sink nodes to be deployed in the park must be no greater than a maximum capacity number $Q$ as follows:

$$\sum_{i=1}^{N} X_i \leq Q \qquad (6)$$

where $X_i$ is a binary variable to determine whether candidate node $x_i$ is selected to be deployed with a sink node.

Most previous studies on deployment problems of sink nodes have considered collision avoidance, i.e., avoiding that two sink nodes are placed too closely to cause signal collision. Constraint (7) enforces that the distance $D_{ij}$ between two sink nodes deployed on candidate nodes $x_i$ and $x_j$ in the 3D park space must be no less than the given maximum 3D distance MD except that one of the two scores of the two sink nodes is large, as expressed as follows:

$$d(x_i, x_j) \geq X_i \cdot X_j \cdot \lambda_{ij} \cdot \mathrm{MD}, \quad \forall i, j \in \{1, 2, \ldots, N\}, \ i \neq j \qquad (7)$$

where $\lambda_{ij}$ is a binary variable to determine whether at least one of the scores of the two target nodes corresponding to candidate nodes $x_i$ and $x_j$ is no less than threshold $S_{\mathrm{th}}$ (i.e., if the $\lambda_{ij}$ value is zero, the distance constraint between sink nodes is cancelled). This exception is set because we would like the candidate nodes causing larger scores (i.e., higher visitor flows or larger-score crucial facilities) to be

selected to be deployed by sink nodes to share sensing loads. When the sink nodes are collecting data from the wearable devices, they are limited by hardware so that only a limited number of wearable devices can be read at the same time. A high score for tourism attractiveness indicates that this tourism attractiveness region is popular and has high visitor flows. Visitors wear these wearable devices, and thus, regions with higher scores require a larger number of sink nodes to read visitors' wearable devices, in order to prevent sink nodes from being overloaded by an excessive number of wearable devices.

In Constraint (8), the sum of scores of the target nodes covered by each sink node must not exceed an upper bound $U$ as follows:

$$\sum_{k=1}^{T} G_{ki} \cdot S(t_k) \leq U, \quad \forall i \in \{1, 2, \ldots, N\} \qquad (8)$$

where $G_{ki}$ is a binary decision variable to determine whether target node $t_k$ is covered by the sink node deployed on candidate node $x_i$. Note that it is not necessary to add another constraint similar to Constraint (8) for crucial facility nodes, because target nodes include crucial facility nodes.

The constraints used to calculate decision variables $G_{ki}$ and $C_k$ are as follows:

$$(R - d(t_k, x_i)) \cdot G_{ki} \geq 0, \quad \forall k \in \{1, 2, \ldots, T\},$$
$$\forall i \in \{1, 2, \ldots, N\}; \qquad (9)$$
$$C_k = \max_{i \in \{1, 2 \ldots, N\}} \{G_{ki}\}, \quad \forall k \in \{1, 2, \ldots, T\}. \qquad (10)$$

The constraints for all binary variables are as follows:

$$X_i, \lambda_{ij}, C_k, G_{ki} \in \{0, 1\}, \quad \forall k \in \{1, 2, \ldots, T\},$$
$$\forall i \in \{1, 2, \ldots, N\}. \qquad (11)$$

The differences of the model of this study from previous studies are as follows.

- Different from previous studies that focused on 2D deployment of sink nodes in IoT systems, this study investigates 3D deployment.
- Different from previous studies that hardly considered optimization of multiple management indices in forest recreation parks, this study proposes 3D deployment of an IoT system with optimal management service indices (i.e., SQI and MSAI).
- This study considers the deployment problem with coverage, collision avoidance, and maximal reading loads.

Note that the IoT devices are vulnerable to interference in dense forest and hilly areas. To ensure connectivity in these areas, park managers can set the grid nodes within these areas as critical facility nodes with higher scores. Therefore, when the proposed algorithm searches for a deployment with higher scores, it tends to deploy more sink nodes in these vulnerable areas to ensure connectivity.

**Algorithm 1** Proposed ISA

1:  Initialize the current temperature $\tau = \tau_h$
2:  Randomly generate an initial solution $X$, and use
    Algorithm 2 to evaluate the cost $\delta(X)$ of solution $X$
3:  Initialize the probabilities of selecting the insertion
    operator ($\pi_1$), the swap operator ($\pi_2$), and the inversion
    operator ($\pi_3$), i.e., $\pi_1 = \pi_2 = \pi_3 = 1/3$
4:  **while** $\tau > \tau_l$ **do**
5:      **while** the iteration number is no more than dwell
            times $L$ **do**
6:          Use Algorithm 3 to search for a neighboring
                solution $X'$
7:          Use Algorithm 2 to evaluate the cost $\delta(X')$ of the
                neighboring solution $X'$
8:          Use Algorithm 4 to conduct the dynamic
                selection probability adjustment scheme
9:          **if** $(\delta(X') < \delta(X))$ or $(\delta(X') \geq \delta(X)$ and
                $rand(0, 1) < \exp(-(\delta(X') - \delta(X))/(\kappa\tau)))$ **then**
10:             $X = X'$
11:         **end if**
12:     **end while**
13:     Decrease temperature (i.e., $\tau = \tau \cdot \gamma$)
14: **end while**

## IV. PROPOSED ISA FOR THE CONCERNED PROBLEM

The deployment problems of IoT systems have been shown to be NP-hard (e.g., [10], [11]). The problem of this study extends the previous deployment problems, and hence is also NP-hard. Therefore, this study further proposes an ISA to solve the problem. The ISA is a simulated annealing (SA) [37], which is a global optimization metaheuristic algorithm, which can escape from local optimal solutions and allow the user easily adjust the parameters of the algorithm. The idea of the SA is to solve a problem through simulating an annealing process of a solid. First, the SA generates a random solution. Then, it iteratively searches for a neighboring solution of this solution through a temperature cooling scheme, and determines whether the neighboring solution replaces the current solution through the Metropolis criterion. The SA has successfully solved numerous optimization problems.

The proposed ISA improves the SA with two schemes: 1) three neighborhood searching operators, and 2) the dynamic selection probability adjustment scheme. The proposed ISA is given in Algorithm 1, and its flowchart is given in Figure 2. The details of Algorithm 1 are explained as follows. The ISA is operated with a temperature cooling scheme, i.e., decreasing from the highest temperature $\tau_h$ to the lowest temperature $\tau_l$. Therefore, Line 1 first initializes temperature $\tau$ to be the highest temperature $\tau_h$. Subsequently, Line 2 randomly generates an initial solution $X$, and uses Algorithm 2 to evaluate its cost $\delta(X)$.

Different from the SA, the ISA adopts a dynamic selection probability adjustment scheme, which dynamically adjusts the probabilities of selecting three neighborhood searching
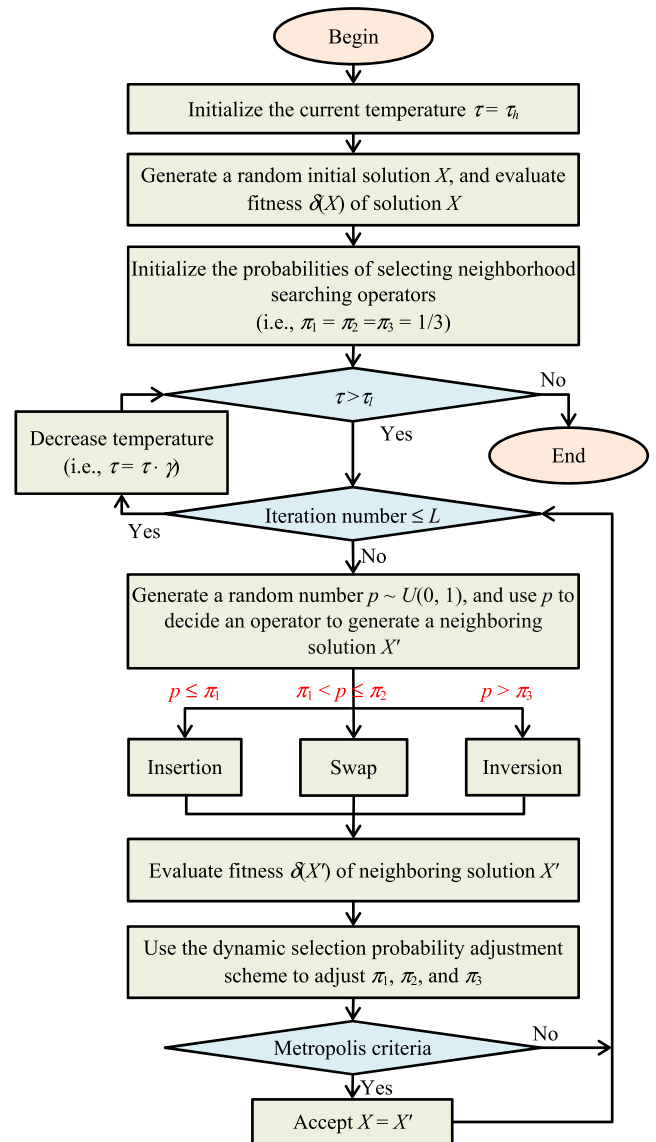


**FIGURE 2.** Flowchart of the proposed ISA.

operators: insertion, swap, and inversion (i.e., $\pi_1, \pi_2$, and $\pi_3$). Initially, Line 3 sets all probabilities to be equal, i.e., $\pi_1 = \pi_2 = \pi_3 = 1/3$. Then, the ISA enters a main loop (Lines 4 – 14) based on a temperature cooling scheme (i.e., the temperature $\tau$ decreases from $\tau_h$ to $\tau_l$, and the ratio of the next temperature and the current temperature is $\gamma$).

Inside the main loop (Lines 4 – 14), the inner loop (Lines 5 – 12) executes at most $L$ iterations (a.k.a., dwell times) under a fixed temperature $\tau$. In the inner loop, a neighboring solution is generated by Algorithm 3 (Line 6), which selects one of the three neighborhood searching operators according to probabilities $\pi_1, \pi_2$, and $\pi_3$. Line 7 uses Algorithm 2 to evaluate the cost $\delta(X')$ of the neighboring solution $X'$. Then, Line 8 uses Algorithm 4 to conduct the dynamic selection probability adjustment scheme. Then, Line 9 checks the Metropolis criterion. If the criterion is true, then Line 10 replaces the current solution $X$ by the

**Algorithm 2** Cost Evaluation

**Input:** A solution $X = (X_1, X_2, \ldots, X_N)$
**Output:** Cost of the solution $\delta(X)$.
1: Initialize TCS, TFS, $\rho_{\text{quantity}}$, $\rho_{\text{distance}}$, $\rho_{\text{terrain}}$, and $\rho_{\text{score}}$ to be zero.
2: **for each** $k = 1, 2, \ldots, T$ **do**
3:      **for each** $i = 1, 2, \ldots, N$ **do**
4:          **if** $d(t_k, x_i) < R$ **then**
5:             $G_{ki} = 1$
6:          **else**
7:             $G_{ki} = 0$
8:          **end if**
9:      **next for**
10:      $C_k = \max_{i \in \{1, 2 \ldots, N\}} G_{ki}$
11: **next for**
12: **for each** $k = 1, 2, \ldots, T$ **do**
13:      **if** $C_k = 1$ **then**
14:          $\text{TCS} = \text{TCS} + S(t_k)$
15:      **end if**
16: **next for**
17: **for each** $l = 1, 2, \ldots, F$ **do**
18:      **if** $C_{\mu(f_l)} = 1$ **then**
19:          $\text{TFS} = \text{TFS} + S(f_l)$
20:      **end if**
21: **next for**
22: $\rho_{\text{quantity}} = \max\{\sum_{i=1}^{N} X_i - Q, 0\}$
23: **for each** $i = 1, 2, \ldots, N - 1$ **do**
24:      **for each** $j = i + 1, \ldots, N$ **do**
25:          **if** $S(X_i) < S_h$ and $S(X_j) < S_{\text{th}}$ and $X_i = 1$ and $X_j = 1$ and $d(x_i, x_j) < \text{MD}$ **then**
26:             $\rho_{\text{terrain}} = \rho_{\text{terrain}} + 1$
27:      **next for**
28: **next for**
29: **for each** $i = 1, 2, \ldots, N$ **do**
30:      **if** $\sum_{k=1}^{T} G_{ki} \cdot S(t_k) > U$ **then**
31:          $\rho_{\text{score}} = \rho_{\text{score}} + 1$
32:      **end if**
33: **next for**
34: Output $1 - \omega \cdot \text{TCS} / \sum_{k=1}^{T} S(t_k) \cdot \text{MD} / R - (1 - \omega) \cdot \text{TFS} / \sum_{l=1}^{F} S(f_l) + M_h \cdot (\rho_{\text{qantity}} + \rho_{\text{terrain}}) + M_s \cdot \rho_{\text{score}}$

---

**Algorithm 3** Neighborhood Search

**Input:** A solution $X = (X_1, X_2, \ldots, X_N)$
**Output:** A neighboring solution $X'$
1: Randomly select two numbers $i$ and $j$ from $\{1, 2, \ldots, N\}$ where $i < j$
2: Generate a random value $p$ from the uniform distribution of $[0, 1]$
3: $X' = X$
4: **if** $p \leq \pi_1$ **then**
5:      Move $X_j$ to the $(i - 1)$-th position on solution $X'$
6: **else if** $p \leq \pi_2$ **then**
7:      Swap $X_i$ with $X_j$ on solution $X'$
8: **else**
9:      Reverse the sequence between positions $i$ and $\min\{i + \varepsilon, j\}$ on solution $X'$
10: **end if**

---

deployed with a sink node. Therefore, a solution used in the ISA is encoded as a vector of these decision variables: $(X_1, X_2, \ldots, X_N)$, where $X_i \in \{0, 1\}$.

### B. COST EVALUATION

The ISA requires a cost function to evaluate the performance of the solution. Because the concerned problem is to maximize Objective (1) under major constraints (6)–(8), this study changes to minimize one minus Objective (1), and considers the costs of penalizing violation of the constraints. Note that Constraints (6) and (7) are hard constraints (because their violation leads to infeasibility of the solution); Constraint (8) is a soft constraint (because violation of this constraint only leads to heavy load of sink nodes, but the solution is still feasible). In general, the penalty cost for hard constraints is greater than that for soft constraints. Given a solution $X = (X_1, X_2, \ldots, X_N)$, this study sets the cost $\delta(X)$ of solution $X$ as one minus Objective (1) plus the penalty costs of Constraints (6)–(8) as follows:

$$\delta(X) = 1 - \omega \cdot \text{SQI} - (1 - \omega) \cdot \text{MSAI}$$
$$+ M_h \cdot (\rho_{\text{quantity}} + \rho_{\text{terrain}}) + M_s \cdot \rho_{\text{score}} \quad (12)$$

where $M_h$ (resp., $M_s$) are the costs of penalizing a hard constraint (resp., soft constraint); $\rho_{\text{quantity}}$, $\rho_{\text{terrain}}$, and $\rho_{\text{score}}$ are the numbers of penalizing Constraints (6), (7), and (8), respectively.

The algorithm of evaluating the cost of a solution is given in Algorithm 2, which is explained as follows. Line 1 initializes variables TCS, TFS, $\delta_1$, $\delta_2$, $\rho_{\text{quantity}}$, $\rho_{\text{distance}}$, $\rho_{\text{terrain}}$, and $\rho_{\text{score}}$ to be zero. Lines $2 - 11$ calculate decision variable $G_{ki}$, which is one only when $d(t_k, x_i) < R$, and further calculate decision variable $C_k = \max i \in \{1, 2 \ldots, N\} G_{ki}$. With the two types of decision variables, Lines $12 - 16$ calculate TCS, and Lines $17 - 21$ calculate TFS. Lines 22 calculates penalty number $\rho_{\text{quantity}}$ for Constraint (6). Lines $23 - 28$ calculate penalty number $\rho_{\text{terrain}}$ for Constraint (7). Lines $29 - 33$ calculate penalty number $\rho_{\text{score}}$ for Constraint (8). Finally, Lines 34 calculates the cost according to Equation (12).

neighboring solution $X'$. The main function of the Metropolis criterion is to escape from a local optimal solution and prevent premature convergence. The criterion include the following two cases: (1) If the neighboring solution $X'$ is better than the current solution $X$ (i.e., $\delta(X') < \delta(X)$), then it accepts $X'$. (2) If the neighboring solution $X'$ is worse (i.e., $\delta(X') \geq \delta(X)$), then it still accepts $X'$ when a random number between 0 and 1 is smaller than $\exp(-(\delta(X') - \delta(X))/(\kappa\tau))$, which a Boltzmann distribution, where $\kappa$ is the Boltzmann constant.

### A. SOLUTION REPRESENTATION

As detailed in the last section, the decision variables of the problem model are $X_1, X_2, \ldots, X_N$, where $X_i$ is a binary variable to determine whether the $i$th candidate node is

---

**Algorithm 4** Dynamic Selection Probability Adjustment Scheme

1: **if** $\delta(X') < \delta(X)$ **then**
2:  Compute $\Delta v_1$ by Equation (15)
3:  **if** the insertion move is adopted **then**
4:   $\pi_1 = \pi_1 + \Delta v_1$
5:   $\pi_2 = \pi_2 - \Delta v_1/2$ and $\pi_3 = \pi_3 - \Delta v_1/2$
6:  **else if** the swap move is adopted **then**
7:   $\pi_2 = \pi_2 + \Delta v_1$
8:   $\pi_1 = \pi_1 - \Delta v_1/2$ and $\pi_3 = \pi_3 - \Delta v_1/2$
9:  **else**
10:   $\pi_3 = \pi_3 + \Delta v_1$
11:   $\pi_1 = \pi_1 - \Delta v_1/2$ and $\pi_2 = \pi_2 - \Delta v_1/2$
12:  **end if**
13: **else**
14:  Compute $\Delta v_2$ by Equation (16)
15:  **if** the insertion move is adopted **then**
16:   $\pi_1 = \pi_1 + \Delta v_2$
17:   $\pi_2 = \pi_2 - \Delta v_2/2$ and $\pi_3 = \pi_3 - \Delta v_2/2$
18:  **else if** the swap move is adopted **then**
19:   $\pi_2 = \pi_2 + \Delta v_2$
20:   $\pi_1 = \pi_1 - \Delta v_2/2$ and $\pi_3 = \pi_3 - \Delta v_2/2$
21:  **else**
22:   $\pi_3 = \pi_3 + \Delta v_2$
23:   $\pi_1 = \pi_1 - \Delta v_2/2$ and $\pi_2 = \pi_2 - \Delta v_2/2$
24:  **end if**
25: **end if**
26: **for** $s = 1, 2, 3$ **do**
27:  **if** $\pi_s > 0.8$ **then**
28:   $\pi_s = 0.8$
29:   $\pi_t = \pi_t + (\pi_s - 0.8)/2$ for each
    $t \in \{1, 2, 3\} \setminus \{s\}$
30:  **else if** $\pi_s < 0.1$ **then**
31:   $\pi_s = 0.1$
32:   $\pi_t = \pi_t + (0.1 - \pi_s) / 2$ for each
    $t \in \{1, 2, 3\} \setminus \{s\}$
33:  **end if**
34: **next for**

---

### C. THREE NEIGHBORHOOD SEARCHING OPERATORS

Each iteration of the ISA generates a neighboring solution $X'$ of the current solution $X$ (i.e., Line 6 of Algorithm 1), based on three neighborhood searching operators [38] (Figure 3):

- Insertion: This operator refers to randomly selecting one element in the solution vector $X$, and then inserting this element before another randomly selected location.
- Swap: This operator refers to randomly selecting two elements from solution $X$, and then swapping them.
- Inversion: This operator refers to randomly selecting two indices from $\{1, 2, \ldots, N\}$. Subsequently, the subsequence of solution $X$ between the two indices is reversed. To avoid excessively large changes in the generated neighboring solution, the maximum length of inversion is set as $\varepsilon$.
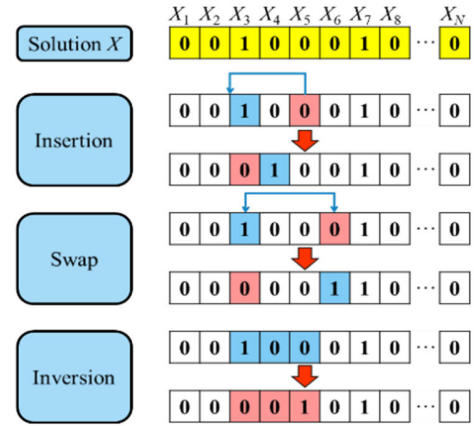


**FIGURE 3.** Illustration of three neighborhood searching operators.

The proposed ISA conducts the above three neighborhood searching operators according to three probability values adjusted in each iterations (i.e., $\pi_1$, $\pi_2$, $\pi_3$). The algorithm of generating a neighboring solution is presented as Algorithm 3.

### D. DYNAMIC SELECTION PROBABILITY ADJUSTMENT SCHEME

The proposed ISA employs a dynamic selection probability adjustment scheme [39] to dynamically change the probabilities of selecting three neighborhood searching operators (i.e., $\pi_1$, $\pi_2$, $\pi_3$) according to performance of their respective cost values. The algorithm of the dynamic selection probability adjustment scheme is presented as Algorithm 4. The initial values of $\pi_1$, $\pi_2$, and $\pi_3$ are set equally as 1/3 (Line 3 of Algorithm 1). After obtaining the neighboring solution $X'$ of the current solution $X$, Algorithm 4 compares the cost values of the two solutions. If the neighboring solution is better (i.e., $\delta(X') < \delta(X)$), then Line 2 computes a normalized cost variation $\Delta v_1$ as follows:

$$\Delta v_1 = (\delta(X) - \delta(X'))/(\delta(X) + \delta(X')) \tag{13}$$

Let $s$ denote the index of the neighborhood searching operator selected in this iteration of the ISA. Then, based on $\Delta v_1$, Lines 3 – 12 adjust the three probabilities as follows:

$$\pi_s = \pi_s + \Delta v_1, \quad \forall s \in \{1, 2, 3\}; \tag{14}$$
$$\pi_h = \pi_h - \Delta v_1/2, \quad \forall h \in \{1, 2, 3\}, \ h \neq s. \tag{15}$$

That is, the probability of selecting operator $s$ increases with $\Delta v_1$, while the other two probabilities decrease with $\Delta v_1/2$. With the above adjustment, the probability of selecting operator $s$ will be higher in the next iteration of the ISA, while the probabilities of selecting other two operators will be lower.

If the cost value of the neighboring solution is not better than that of the current solution (i.e., $\delta(X') \geq \delta(X)$), then Lines 14 – 24 also adjust the three probabilities similarly, but the variation is scaled with a ratio $\alpha$ between 0 and 1 as

follows:

$$\Delta v_2 = (\delta(X') - \delta(X))/(\delta(X) + \delta(X')) \cdot \alpha; \quad (16)$$

$$\pi_s = \pi_s + \Delta v_2, \quad \forall s \in \{1, 2, 3\}; \quad (17)$$

$$\pi_h = \pi_h - \Delta v_2/2, \quad \forall h \in \{1, 2, 3\}, \ h \neq s. \quad (18)$$

Finally, to avoid an overly large or small probability of a certain operator and the results tending toward a single operator, we set an upper bound of 0.8 and a lower bound of 0.1. When the probability of the selected operator $s$ is larger than 0.8, it is maintained at 0.8, whereas when this probability is less than 0.1, it would is at 0.1. Lines $26 - 34$ conduct the adjustments based on the values of 0.8 and 0.1, which is similar to the above adjustment schemes.

In light of the above, the proposed dynamic selection probability adjustment scheme is not a greedy approach.

Note that different from the SA, the ISA additionally adopts Algorithm 4 and mathematical equations (13) – (18).

Also note that in general, the deployment of IoT sink nodes is not modified frequently after these nodes are deployed in the park. Once the environment of the park is changed due to natural calamities (such as storm, flood, and mist), the park managers can execute the proposed algorithm to generate a new deployment of sink nodes to adapt to the environment change, and then they adjust the existing deployment of sink nodes according to the new deployment result.

## V. EXPERIMENTAL RESULTS AND ANALYSIS

Based on the ISA detailed in the last section, this section implements the ISA, conducts simulation, and compares experimental results. This section first gives the experimental setting and environment, then analyzes the parameters used in the ISA, then compares experimental results using different approaches, then analyzes the weight of SQI in the objective function, then analyzes various minimal distances between sink nodes, and finally analyzes the effect of canceling the score threshold in the distance constraint between sink nodes.

### A. EXPERIMENTAL SETTING AND ENVIRONMENT

The experiments in this section is conducted on a PC with an Intel Core$^{\text{TM}}$ i7-7700CPU @ 3.60GHz CPU and memory of 8 GB. The study area is the Huisun Forest Recreation Area (HFRA) in Taichung, Taiwan, which has an area of 7477 hectares, and whose altitude is between 450 and 2419 meters. This study divides the major area of the HFRA into $14 \times 22$ grids (Figure 4(a)); each of these grid points has a 3D coordinate, and the side length of each grid is 100 meters. Figure 4(b) presents a simplified map of the HFRA; the green area is inside the HFRA, and the white area is not. Cooperated with the HFRA staff, we collected single-day visitor flows of the HFRA, and determined the importance of the tourism attractiveness of each tourist attraction within the park; different scores were assigned to different grids (see the number labeled on each grid in Figure 4(b)) according to visitor flows in Table 3. Then, we adjusted these scores according to crucial facilities. Figure 5(a) shows target nodes
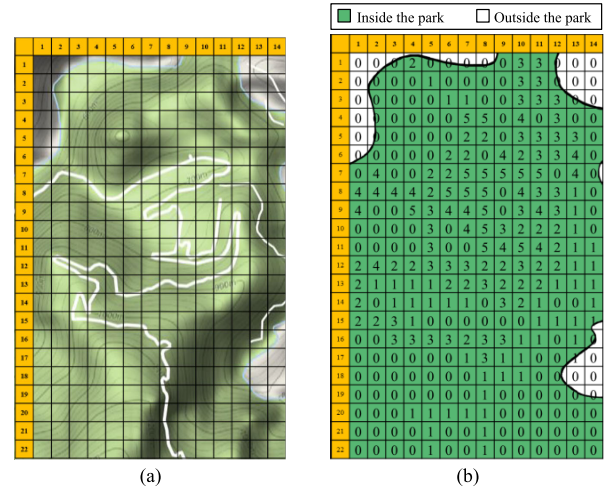


**FIGURE 4.** (a) The HFRA map (with contour lines) is divided into 14 × 22 grids, and the length of each 2D grid is 100 meters. (b) A simplified HFRA map, in which each grid is attached with a score number according to visitor flow.

**TABLE 3.** Relation between one-day visitor flows and scores.

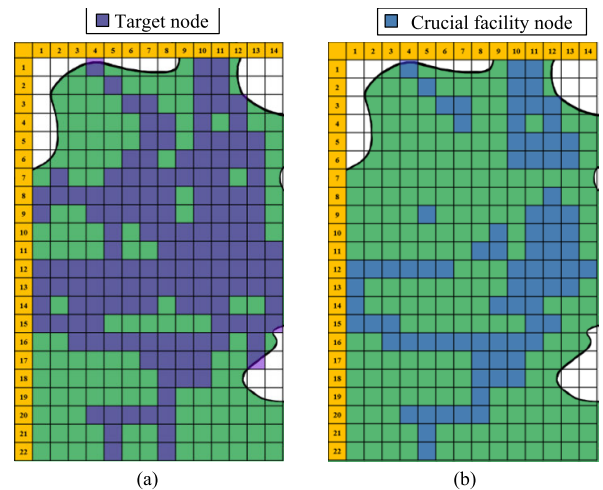| One-day visitor flow | $\leq 20$ | 21-25 | 26-30 | 31-35 | 36-40 | $\geq 41$ |
|---|---|---|---|---|---|---|
| Score | 0 | 1 | 2 | 3 | 4 | 5 |



**FIGURE 5.** (a) Distribution of target nodes in the HFRA. (b) Distribution of crucial facility nodes in the HFRA.

colored in purple, and Figure 5(b) shows crucial facility nodes colored in blue.

Based on the case of the HFRA, the experimental parameters are set as follows. This study first assumes that the MSAI is as important as the SQI (i.e., $\omega = 0.5$). The coverage radius $R$ of each sink node is 150 meters, and the maximal score sum $U$ of all target nodes covered by a sink node is 30. The minimum distance MD between sink nodes is 240 meters. Based on the data of the HFRA, we decide that the target nodes, candidate nodes, and the crucial facility nodes emphasized by managers which include toilets, specific tourist attractions,

and specific trails. The other parameters are set as follows: $Q = 20$, $M_h = 100$, $M_s = 10$, $S_{th} = 5$, and $\alpha = 0.5$.

As mentioned in Section 1, most studies focused on deployment of the IoT system that optimizes various objectives unrelated to management service benefits, but this study considers the objective with optimal management service benefits. Most studies investigated deployment of IoT systems in 2D spaces, regardless of actual 3D topographic differences, but this study considers 3D deployment of IoT systems. Most studies assumed all targets to be equally crucial, but this study considers that the importance of each target may be different. Most studies rarely investigated the service level index, but this study does. As a consequence, the experimental results of the proposed approach are compared with previous studies.

## B. ANALYSIS ON ALGORITHMIC PARAMETERS

This subsection analyzes the experimental results under various settings of the parameters of the proposed ISA, including the Boltzmann constant $\kappa$, highest temperature $\tau_h$, lowest temperature $\tau_l$, dwell times $L$, and temperature-cooling scale $\gamma$; additionally, and the maximal length $\varepsilon$ of the substring adopted in the inversion neighborhood searching operator. In Table 4, each statistical value is obtained from 20 experiments under different combinations of parameters $L$, $\gamma$, and $\varepsilon$. Based on the results in Table 4, the ISA parameters in the later experimental results are set as follows: $\kappa = 1/5$, $\tau_h = 1000$, $\tau_l = 10$, $L = 500$, $\gamma = 0.99$, and $\varepsilon = 20$.

**TABLE 4.** Experimental analysis of the parameters used in the proposed ISA.

| $L$ | $\gamma$ | $\varepsilon$ | Cost | | |
|---|---|---|---|---|---|
| | | | Best | Average | StdDev |
| 300 | 0.96 | 20 | 7460.208 | 16166.131 | 4867.207 |
| | | 40 | 5960.255 | 13012.142 | 5123.605 |
| | 0.97 | 20 | 3840.161 | 10121.150 | 4070.888 |
| | | 40 | 3050.197 | 7387.176 | 2605.565 |
| | 0.98 | 20 | 0.305 | 1604.275 | 1277.112 |
| | | 40 | 0.347 | 1378.786 | 1472.704 |
| | 0.99 | 20 | 0.352 | 0.380 | 0.029 |
| | | 40 | 0.329 | 0.378 | 0.031 |
| 400 | 0.96 | 20 | 4360.159 | 10308.147 | 4639.769 |
| | | 40 | 5760.210 | 10582.649 | 4464.970 |
| | 0.97 | 20 | 800.333 | 4840.691 | 2372.162 |
| | | 40 | 0.391 | 3055.739 | 2012.864 |
| | 0.98 | 20 | 0.308 | 115.359 | 296.054 |
| | | 40 | 0.333 | 308.342 | 789.790 |
| | 0.99 | 20 | 0.277 | 0.367 | 0.029 |
| | | 40 | 0.339 | 0.390 | 0.034 |
| 500 | 0.96 | 20 | 900.406 | 5922.679 | 3528.033 |
| | | 40 | 800.339 | 4897.209 | 3555.744 |
| | 0.97 | 20 | 0.286 | 1963.769 | 1862.279 |
| | | 40 | 0.329 | 719.327 | 863.055 |
| | 0.98 | 20 | 0.329 | 0.366 | 0.023 |
| | | 40 | 0.318 | 0.368 | 0.026 |
| | **0.99** | **20** | **0.304** | **0.360** | **0.030** |
| | | 40 | 0.326 | 0.368 | 0.027 |

## C. EXPERIMENTAL COMPARISON OF DIFFERENT APPROACHES

This subsection analyzes experimental results using three different approaches: (1) classical SA, (2) multi-search

simulated annealing (MSA) with three neighbor searching operators (i.e., the ISA without the dynamic selection probability adjustment scheme, so that the three operators are selected with an equal probability), and (3) the proposed ISA (including three neighbor searching operators and the dynamic selection probability adjustment scheme). This enables us to gain knowledge of whether superior performance could be found in the results after different mechanisms are incorporated.

**TABLE 5.** Comparison of the experimental results using different approaches.

| Approach | Best | Average | Worst | StdDev | Time (s) |
|---|---|---|---|---|---|
| SA | 0.6044 | 272.8813 | 2200.8958 | 509.1113 | 38.7109 |
| MSA | 0.3178 | 0.3844 | 0.4748 | 0.0331 | 37.9846 |
| ISA | 0.3101 | 0.3705 | 0.4594 | 0.0306 | 150.5832 |

Table 5 shows the best, average, and worst cost values as well as the standard deviation and mean computation time for executing SA, MSA, and ISA 50 times. Some of the SA results include feasible solutions. The best cost value of the proposed ISA is 0.3101, which is superior to those of SA and MSA. In terms of the average and worst cost values and standard deviation, the proposed ISA still exhibits superior performance. In terms of mean computation time, it is reasonable that the proposed ISA takes much more CPU time. To observe the stability of the three approaches, each of the three approaches are executed 50 times. Figure 6 indicates that both MSA and ISA have high stability and feasibility, as well as that ISA has superior performance overall.
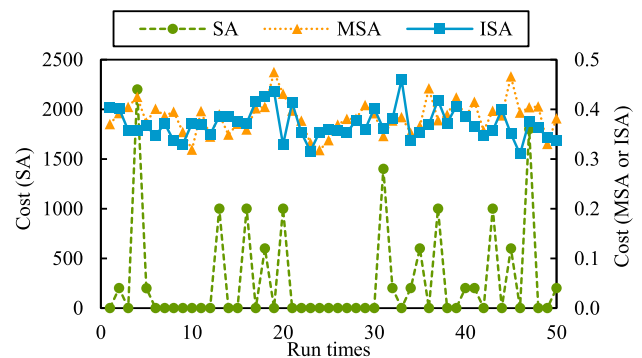


**FIGURE 6.** Comparison of the results of executing each of three approaches 50 times.

Figure 7 shows the convergence results of executing three approaches. In terms of convergence speeds, both SA and MSA are faster than ISA. However, in terms of the ability to search for optimal solutions, a comparison of final cost values indicates that the cost value for SA was 0.9151, that for MSA was 0.6754, and that for ISA was 0.3403, demonstrating that the proposed ISA has superior cost value. Figure 8 shows box plots, respectively, for executing SA, MSA, and ISA 50 times each. In terms of cost comparison, the experimental results of ISA are superior those of SA and MSA.
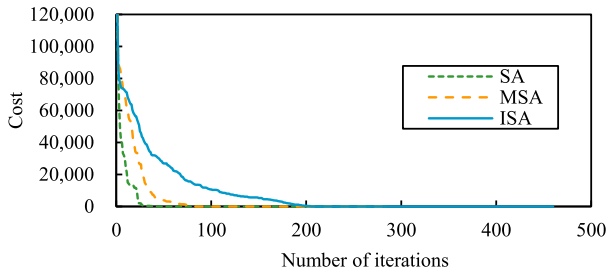
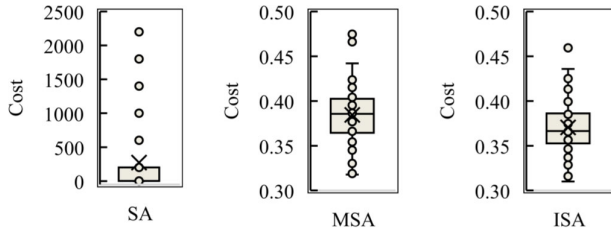**FIGURE 7.** Convergence results of executing three approaches.



**FIGURE 8.** Box plot for executing SA, MSA, and ISA 50 times each.

### D. ANALYSIS ON THE WEIGHT OF SQI IN THE OBJECTIVE FUNCTION

The weight $\omega$ of the SQI determines the importance degree of the SQI to which the park managers emphasize, as compared with the MSAI. To observe how different values of the SQI weight $\omega$ would affect the deployment results, weight $\omega$ is set under 0.1 and 0.9, and the deployment results of 20 sink nodes are presented in Figures 9(a) and 9(b), respectively. When the weight $\omega$ of the SQI is 0.1, this indicates that the weight $(1 - \omega)$ of the MSAI is 0.9. The blue grids represent crucial facility grids emphasized by park managers, which are nearly covered by sink nodes (Figure 9(a)). When the weight $\omega$ of the SQI is 0.9, this indicates that the weight $(1 - \omega)$ of
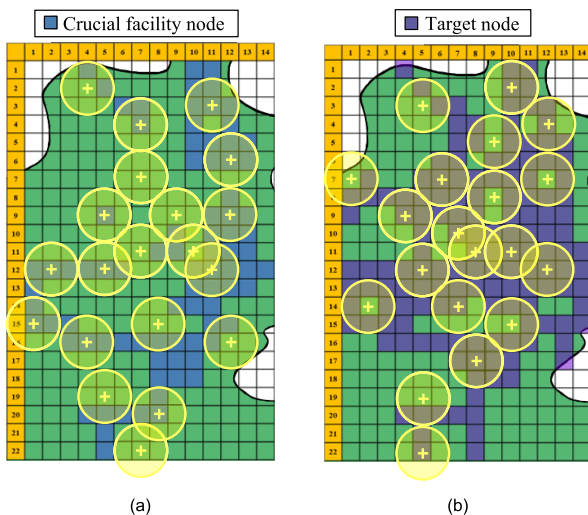


**FIGURE 9.** The experimental results of deploying sink nodes in the HFRA when (a) $\omega = 0.1$ and (b) $\omega = 0.9$.

the MSAI is 0.1; the purple grids represent the target nodes (i.e., those with visitor flows), which are nearly covered by sink nodes (Figure 9(b)).

### E. ANALYSIS ON VARIOUS MINIMAL DISTANCES BETWEEN SINK NODES

The setting of the minimal distance between the sink nodes (MD) affects the distance between two adjacent sink nodes. Figures 10(a) and 10(b) set MD as 100 and 270 meters, respectively, and present the deployment results of 20 sink nodes. In the two figures, the 2D grid has a side length of 100 meters and a sink-node coverage radius of 150 meters. When MD is 100 meters, this means that the distance between adjacent sink nodes is allowed to be short, resulting in dense overall deployment results (Figure 10(a)). However, when MD is 270 meters, this indicates that the distance between adjacent sink nodes is allowed to be long, resulting in a more dispersed overall deployment result (Figure 10(b)).
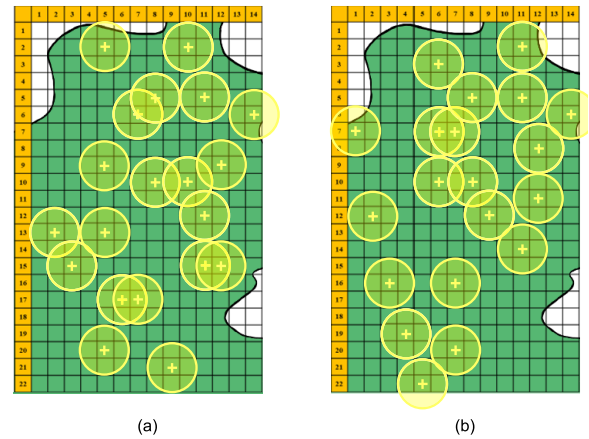


**FIGURE 10.** The experimental results of deploying sink nodes in the HFRA when (a) MD = 100 and (b) MD = 270.

### F. ANALYSIS ON THE SCORE THRESHOLD CANCELING THE DISTANCE CONSTRAINT BETWEEN SINK NODES

When the score threshold in the distance constraint between sink nodes ($S_{th}$) is set as 3, the deployment of sink nodes on grids with scores 3, 4, and 5 is not restricted to the MD, as shown in Figure 11(a). We have checked that the 3D distance between any two grids labeled by numbers in Figure 11(a) is less than the MD, which is set as 240. That is, the MD constraint is canceled for higher-score grids. When $S_{th}$ is set as 5, the deployment of sink nodes on grids with score 5 is not restricted to the MD, as shown in Figure 11(b). We have checked that the 3D distance between any two grids labeled by '5' in Figure 11(a) is less than the MD, which is set as 240.

Figure 4(a) shows the actual 3D topographic differences of the study area, in which the dark areas represent the steep mountainside; the blue curve represents a surrounding river; the white curve represents a winding road; and the contour lines of mountains are illustrated. From the visualization of
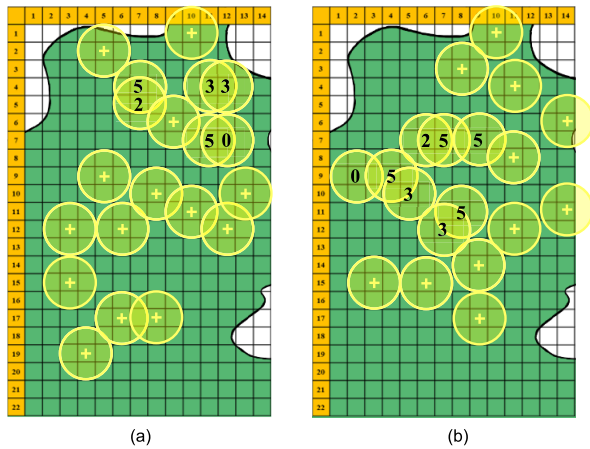
**FIGURE 11.** The experimental results of deploying sink nodes in the HFRA when (a) $S_{th} = 3$ and (b) $S_{th} = 5$.

all the experimental results (Figures 9–11), we observe that the environment factors influence the results (e.g., the mountainside areas without target nodes and crucial facility nodes are not deployed with sink nodes; and rivers are not deployed as well); the deployment is noised by artificial constructions (e.g., because crucial facilities are constructed along the artificial winding road, sink nodes tend to be deployed along the winding road).

## VI. CONCLUSION

This study has proposed an ISA algorithm to solve the problem of deploying an IoT system to cover targets with different scores based on tourist attractiveness in a 3D forest recreation park with optimal service benefits, which is represented as a weighted sum of SQI and MSAI, which could help forest park managers to evaluate the quality of their IoT deployments and their deployment needs. The proposed ISA includes three neighborhood searching operators, and the probabilities of these operators are adjusted by a dynamic selection probability adjustment scheme. Through simulation, the proposed ISA was found to have excellent ability in searching for solutions. Specifically, the optimal deployment location of sink nodes was determined in a manner that facilitated satisfying the deployment needs of forest creation park managers, thereby maximizing managerial service benefits. Moreover, this study provides a reference to forest recreation park managers who wish to integrate smart tourism management through introducing an IoT system. However, the range of applications is not limited to forest parks; it can also be introduced to theme parks, water parks, and large outdoor playgrounds.

Future studies can be extended in the following directions. First, the locations where sink nodes are placed should be continuous and must not be limited by the location of candidate nodes, which would enable actual deployment locations to be more precise. Furthermore, because forest recreation parks would have different landscapes during different seasons, special festivals can be held to change visitor flows.

This would allow for the dynamic adjustment of tourist attraction scores according to seasons and times. Sink nodes are heterogeneous, and different device functions have different sensing radii. Their sensing state is to start, sleep, malfunction, and die, which can be scheduled according to the coverage conditions. In addition, this work does not consider communication of visitors under water, because it is related with a different sensor type such as underwater acoustic sensors [40]. It would be of future interest to investigate the heterogeneous IoT system with underwater acoustic sensors. Furthermore, some location-based recommendation methods (e.g., [41], [42]) may be considered to be incorporated with the proposed approach in the future.

## REFERENCES

[1] J. Gubbi, R. Buyya, S. Marusic, and M. Palaniswami, "Internet of Things (IoT): A vision, architectural elements, and future directions," *Future Generat. Comput. Syst.*, vol. 29, no. 7, pp. 1645–1660, 2013.

[2] U. Gretzel, M. Sigala, Z. Xiang, and C. Koo, "Smart tourism: Foundations and developments," *Electron. Markets*, vol. 25, no. 3, pp. 179–188, 2015.

[3] D. Z. Jovicic, "From the traditional understanding of tourism destination to the smart tourism destination," *Current Issues Tourism*, vol. 22, no. 3, pp. 276–282, 2019.

[4] E. Mäntymaa, V. Ovaskainen, A. Juutinen, and L. Tyrväinen, "Integrating nature-based tourism and forestry in private lands under heterogeneous visitor preferences for forest attributes," *J. Environ. Planning Manage.*, vol. 61, no. 4, pp. 724–746, 2018.

[5] S. Sengupta, S. Das, M. D. Nasir, and B. K. Panigrahi, "Multi-objective node deployment in WSNs: In search of an optimal trade-off among coverage, lifetime, energy consumption, and connectivity," *Eng. Appl. Artif. Intell.*, vol. 26, no. 1, pp. 405–416, 2013.

[6] I. F. Akyildiz, W. Su, Y. Sankarasubramaniam, and E. Cayirci, "A survey on sensor networks," *IEEE Commun. Mag.*, vol. 40, no. 8, pp. 102–114, Aug. 2002.

[7] C. Y. Tsai, H. T. Chang, and R. J. Kuo, "An ant colony based optimization for RFID reader deployment in theme parks under service level consideration," *Tourism Manage.*, vol. 58, pp. 1–14, Feb. 2017.

[8] D. W. Engels and S. E. Sarma, "The reader collision problem," in *Proc. IEEE Int. Conf. Syst., Man Cybern. (SMC)*, Oct. 2002, p. 6.

[9] F. Campioni, S. Choudhury, and F. Al-Turjman, "Scheduling RFID networks in the IoT and smart health era," *J. Ambient Intell. Humanized Comput.*, vol. 10, no. 10, pp. 4043–4057, Oct. 2019.

[10] Y. J. Gong, M. Shen, J. Zhang, O. Kaynak, W. N. Chen, and Z. H. Zhan, "Optimizing RFID Network Planning by Using a Particle Swarm Optimization Algorithm With Redundant Reader Elimination," *IEEE Trans Ind. Informat.*, vol. 8, no. 4, pp. 900–912, Nov. 2012.

[11] S. Tang, C. Wang, X. Y. Li, and C. Jiang, "Reader activation scheduling in multi-reader RFID systems: A study of general case," in *Proc. IEEE Int. Parallel Distrib. Process. Symp.*, May 2011, pp. 1147–1155.

[12] M. Rebai, M. Le Berre, H. Snoussi, F. Hnaien, and L. Khoukhi, "Sensor deployment optimization methods to achieve both coverage and connectivity in wireless sensor networks," *Comput. Oper. Res.*, vol. 59, pp. 11–21, Jul. 2015.

[13] I. Khoufi, P. Minet, A. Laouiti, and S. Mahfoudh, "Survey of deployment algorithms in wireless sensor networks: Coverage and connectivity issues and challenges," *Int. J. Auton. Adapt. Commun. Syst.*, vol. 10, no. 4, pp. 341–390, 2017.

[14] A. Maheshwari and N. Chand, "A survey on wireless sensor networks coverage problems," in *Proc. 2nd Int. Conf. Commun., Comput. Netw.* (Lecture Notes in Networks and Systems), vol. 46. Singapore: Springer, 2019, pp. 153–164.

[15] M. Farsi, M. A. Elhosseini, M. Badawy, H. Arafat, and H. ZainEldin, "Deployment techniques in wireless sensor networks, coverage and connectivity: A survey," *IEEE Access*, vol. 7, pp. 28940–28954, 2019.

[16] S. Mini, S. K. Udgata, and S. L. Sabat, "Sensor deployment in 3-D terrain using artificial bee colony algorithm," in *Proc. Int. Conf. Swarm, Evol., Memetic Comput. (SEMCCO)* (Lecture Notes in Computer Science), vol. 6466. Singapore: Springer, 2010, pp. 424–431.

[17] S. Mini, S. K. Udgata, and S. L. Sabat, "Sensor deployment and scheduling for target coverage problem in wireless sensor networks," *IEEE Sensors J.*, vol. 14, no. 3, pp. 636–644, Mar. 2014.

[18] L. Sitanayah, "Robust sensor network deployment with priority based on failure centrality," in *Proc. 10th Int. Conf. Inf. Technol. Electr. Eng. (ICITEE)*, Jul. 2018, pp. 175–180.

[19] S. Abdollahzadeh and N. J. Navimipour, "Deployment strategies in the wireless sensor network: A comprehensive review," *Comput. Commun.*, vol. 91, pp. 1–16, Oct. 2016.

[20] L. Hervert-Escobar, N. R. Smith, T. I. Matis, and C. Vargas-Rosales, "Optimal location of RFID reader antennas in a three dimensional space," *Ann. Oper. Res.*, vol. 258, no. 2, pp. 815–823, 2017.

[21] M. S. Lin, J. S. Leu, K. H. Li, and J. L. C. Wu, "Zigbee-based Internet of Things in 3D terrains," *Comput. Electr. Eng.*, vol. 39, no. 6, pp. 1667–1683, 2013.

[22] B. Cao, J. Zhao, Z. Lv, X. Liu, X. Kang, and S. Yang, "Deployment optimization for 3D industrial wireless sensor networks based on particle swarm optimizers with distributed parallelism," *J. Netw. Comput. Appl.*, vol. 103, pp. 225–238, Feb. 2018.

[23] J. Naveen, P. J. A. Alphonse, and S. Chinnasamy, "3D grid clustering scheme for wireless sensor networks," *J. Supercomput.*, to be published.

[24] T. Qasim, M. Zia, Q.-A. Minhas, N. Bhatti, K. Saleem, T. Qasim, and H. Mahmood, "An ant colony optimization based approach for minimum cost coverage on 3-D grid in wireless sensor networks," *IEEE Commun. Lett.*, vol. 22, no. 6, pp. 1140–1143, Jun. 2018.

[25] S. Mnasri, N. Nasri, A. van den Bossche, and T. Val, "Improved many-objective optimization algorithms for the 3D indoor deployment problem," *Arabian J. Sci. Eng.*, vol. 44, no. 4, pp. 3883–3904, 2019.

[26] J. Deng, B. King, and T. Bauer, "Evaluating natural attractions for tourism," *Ann. Tourism Res.*, vol. 29, no. 2, pp. 422–438, 2002.

[27] C. F. Lee, H. I. Huang, and H. R. Yeh, "Developing an evaluation model for destination attractiveness: Sustainable forest recreation tourism in Taiwan," *J. Sustain. Tourism*, vol. 18, no. 6, pp. 811–828, 2010.

[28] T. L. Saaty, "What is the analytic hierarchy process?" in *Math. Models Decision Support*. Berlin, Germany: Springer, 1998, pp. 109–121.

[29] Y. Hu and J. B. Ritchie, "Measuring destination attractiveness: A contextual approach," *J. Travel Res.*, vol. 32, no. 2, pp. 25–34, 1993.

[30] Z. Y. Y. Wang Jin and D. B. Liu Li Zhang, "Comparing social media data and survey data in assessing the attractiveness of Beijing Olympic Forest Park," *Sustainability*, vol. 10, no. 2, 2018, Art. no. 382.

[31] J. Markowski, M. Bartos, A. Rzenca, and P. Namiecinski, "An evaluation of destination attractiveness for nature-based tourism: Recommendations for the management of national parks in Vietnam," *Nature Conservation*, vol. 32, pp. 51–80, Mar. 2019.

[32] O. A. Schipor, R. D. Vatavu, and J. Vanderdonckt, "Euphoria: A Scalable, event-driven architecture for designing interactions across heterogeneous devices in smart environments," *Inf. Softw. Technol.*, vol. 109, pp. 43–59, May 2019.

[33] S. Korpilo, T. Virtanen, and S. Lehvävirta, "Smartphone GPS tracking—Inexpensive and efficient data collection on recreational movement," *Landscape Urban Planning*, vol. 157, pp. 608–617, Jan. 2017.

[34] S. Korpilo, T. Virtanen, T. Saukkonen, and S. Lehvävirta, "More than A to B: Understanding and managing visitor spatial behaviour in urban forests using public participation GIS," *J. Environ. Manage.*, vol. 207, pp. 124–133, Feb. 2018.

[35] S. F. McCool, G. H. Stankey, and R. N. Clark, "Choosing recreation settings: Processes, findings, and research directions," US Forest Service General, Washington, DC, USA, Tech. Rep. INT 184 l-8, 1985.

[36] P. Z. Chen and W. Y. Liu, "Assessing management performance of the national forest park using impact range-performance analysis and impact-asymmetry analysis," *Forest Policy Econ.*, vol. 104, pp. 121–138, Jul. 2019.

[37] N. Metropolis, A. W. Rosenbluth, M. N. Rosenbluth, A. H. Teller, and E. Teller, "Equation of state calculations by fast computing machines," *J. Chem. Phys.* vol. 21, no. 6, pp. 1087–1092, 1953.

[38] S. W. Lin and V. F. Yu, "Solving the team orienteering problem with time windows and mandatory visits by multi-start simulated annealing," *Comput. Ind. Eng.*, vol. 114, pp. 195–205, Dec. 2017.

[39] C. Soza, R. L. Becerra, M. C. Riff, and C. A. C. Coello, "Solving timetabling problems using a cultural algorithm," *Appl. Soft Comput.*, vol. 11, no. 1, pp. 337–344, 2011.

[40] C.-C. Lin, D.-J. Deng, and S.-B. Wang, "Extending the lifetime of dynamic underwater acoustic sensor networks using multi-population harmony search algorithm," *IEEE Sensors J.*, vol. 16, no. 11, pp. 4034–4042, Jun. 2016.

[41] J. Bao, Y. Zheng, D. Wilkie, and M. Mokbel, "Recommendations in location-based social networks: A survey," *GeoInformatica*, vol. 19, no. 3, pp. 525–565, 2015.

[42] W. Luan, G. Liu, C. Jiang, and M. Zhou, "MPTR: A maximal-marginal-relevance-based personalized trip recommendation method," *IEEE Trans. Intell. Transp. Syst.*, vol. 19, no. 11, pp. 3461–3474, Nov. 2018.

**CHUN-CHENG LIN** (S'06–M'08–SM'17) received the B.S. degree in mathematics, the M.B.A. degree in business administration, and the Ph.D. degree in electrical engineering from National Taiwan University, in 2000, 2007, and 2009, respectively. He was an Assistant Professor with the University of Taipei, from 2010 to 2011, and the National Kaohsiung University of Science and Technology, from 2009 to 2010. He has been a Professor with Industrial Engineering and Management, since 2016, and the Associate Dean of the College of Management, National Chiao Tung University, since 2017, where he joined as an Assistant Professor, in 2011. His main research interests include operations research, algorithm, the Internet of Things, and computational management science. He served as a treasure of the IEEE Taipei Section.

**WAN-YU LIU** received the B.B.A. degree in finance from National Chengchi University (NCCU), Taiwan, in 2002, the M.S. degree in agricultural economics and the Ph.D. degree in agricultural economics from National Taiwan University (NTU), Taiwan, in 2004 and 2008, respectively. She then joined the faculty of the Applied Natural Resources Department, Aletheia University (AU), Taiwan. In February 2016, she moved to the Forestry Department, National Chung Hsing University (NCHU), where she is currently a Professor. She has been a Distinguished Professor, since August 2018. Her research interests include forest/farm tourism, environmental economics, and modeling, as well as leisure and recreation.

**YU-WEN LU** received the B.S. degree in industrial engineering and enterprise information from Tunghai University, Taiwan, in 2017, and the M.S. degree in industrial engineering and management from National Chiao Tung University, Taiwan, in 2019. Her main research interests include operations research, metaheuristic algorithms, machine learning, and wireless networks, as well as the Internet of Things.

• • •